Electric Power Systems Research 155 (2018) 254–264

Contents lists available at ScienceDirect

Electric Power Systems Research

journal homepage: www.elsevier.com/locate/epsr

Coordinated control of multifunctional inverters for voltage support and harmonic compensation in a grid-connected microgrid

Seyyed Yousef Mousazade Mousavi [a], Alireza Jalilian [a,b,*], Mehdi Savaghebi [c], Josep M. Guerrero [c]

[a] School of Electrical Engineering, Iran University of Science and Technology, Iran
[b] Center of Excellence for Power System Automation and Operation, Iran University of Science and Technology, Iran
[c] Department of Energy Technology, Aalborg University, Denmark

ARTICLE INFO

Article history:
Received 4 July 2017
Received in revised form
23 September 2017
Accepted 20 October 2017

Keyword:
Distributed generation
Harmonics compensation
DG interfacing inverter
Reactive power compensation

ABSTRACT

In this paper, a coordinated harmonic compensation and voltage support scheme is presented for distributed generations' (DGs') interface inverters in a resistive grid-connected microgrid. Voltage support is performed by reactive power compensation which can mitigate the over/under voltage problem; furthermore, the active power curtailment is proposed in order to mitigate the overvoltage problem when the reactive power compensation is not sufficient. Harmonic compensation is achieved by using virtual admittances in selected harmonic frequencies. Reactive power and harmonic compensation currents are injected with regards to the limited capacity of the interface inverter. If necessary, the reference powers of the grid-tied inverters are changed. Voltage support and harmonic compensation can be achieved based on local or central (communication-based) measurement schemes. The effect of communication delay is also investigated in this study. Experimental and simulation results are obtained in order to demonstrate the effectiveness of the proposed method.

1. Introduction

Voltage Source Inverters (VSIs) are widely used for interfacing Distributed Generation (DG) systems to the grid [1]. The DG interfacing inverters can contribute in voltage support [2–13] and harmonic compensation [12–21] of Microgrids (MGs) and utility grids. These inverters known as multifunctional inverters inject power to the grid and the remaining capacity of the inverter can be dedicated to voltage support and power quality enhancement [10].

To fully comprehend the voltage support of the DG interfacing inverters, reactive power compensation is conventionally proposed in distribution systems [2–7,11,12] and MGs [8–10] in order to mitigate the over/under voltage problems. Overvoltage can be created because of high penetration of Wind Turbine (WT) and Photovoltaic (PV) systems [2]. In Refs. [2,3], the voltage rise problem caused by high penetration of DGs in an LV distribution system has been studied and a droop-based reactive power control is proposed for Current Controlled Mode (CCM) of VSIs. In these papers, the reactive power compensation by DGs interfacing inverters is considered. In Refs. [4,5], the voltage rise mitigation based on active power curtailment in distributed systems has been proposed. The power curtailment algorithms of Refs. [4,5] are based on local measurement and communication system, respectively. In Ref. [6], different reactive power methods for DG units are studied. The reactive power control approaches in Ref. [6] can be classified into distributed and central controller based schemes. The reactive power control of DG interfacing inverters is also studied in Ref. [7]. In this paper, only a grid-connected interfacing inverter is considered whereas in grid-tied MGs more DG units can exist while a coordinated control of the units is required. In Refs. [8,9], voltage and frequency support functions of utility scale PV systems have been proposed. In Ref. [8], the performance of a PV system in voltage sag/swell compensation is evaluated based on the small signal modeling of utility scale PV and power system. In addition, the frequency support is added in Ref. [9]. In Refs. [10,11], the voltage support by Voltage Control Mode (VCM) VSIs in a grid-connected MG has been discussed, while, while it is obvious that, PV and WT systems are integrated as CCM VSIs.

* Corresponding author at: School of Electrical Engineering, Iran University of Science and Technology, Iran.
E-mail addresses: s_y_mosazade@iust.ac.ir (S.Y. Mousazade Mousavi), jalilian@iust.ac.ir (A. Jalilian), mes@et.aau.dk (M. Savaghebi), joz@et.aau.dk (J.M. Guerrero).

https://doi.org/10.1016/j.epsr.2017.10.016
0378-7796/

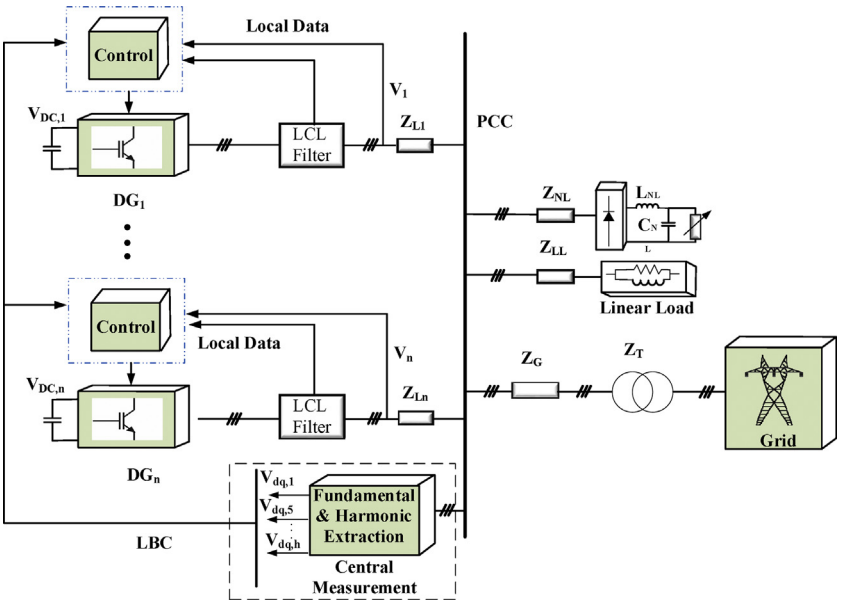

Fig. 1. General overview of the system.

On the other hand, use of DGs interface inverters for compensation of harmonics has been proposed in Refs. [12–22]. The harmonic compensation can be achieved based on communication systems and a central controller [12–17] or local measurement [18–22]. In the communication-based compensation, the data which is used for harmonic compensation is obtained by central controller or measurement whereas in the local compensation; the compensation is achieved without any need for communication systems. In central controller based methods, the compensation can be performed more exactly and more effectively whereas the reliability of the system is decreased and the cost and complexity of the system are increased. The method of Ref. [15] is based on central measurement of Point of Common Coupling (PCC) voltage in a grid-connected MG. In Ref. [15], the harmonic compensation is achieved by central measurement and using VCM VSIs with decentralized controller. In other words, inverters are controlled locally based on the information received from a remote bus. However, in grid-connected MGs, the interfacing VSIs of PV and WT units operate in CCM and their remaining capacity of them (which can be dedicated to harmonic compensation) changes during a day because of the maximum power point variation. The limited capacity of the inverters is not considered in Ref. [15] and the communication system failure can deactivate the harmonics compensation.

Using capacitive virtual impedance which can compensate the harmonic voltage drops of lines and filter impedances has been recommended as a local compensation for VCM VSIs in Refs. [18–20]. Using virtual admittance is recommended for the harmonic compensation by CCM VSIs in distribution system [21] and VCM VSIs in a grid-connected MG [22]. In Refs. [21,22], the control of grid-tied VCM VSI is done by using a fixed value of virtual admittance and local measurement.

In the present paper, a coordinated harmonic compensation and voltage support method are proposed for CCM VSIs in a grid-tied MG. A weak MG with high resistance is chosen as a case study. A voltage support approach with local and central measurement of PCC voltage is proposed in this paper. The voltage support algorithm can mitigate under/over voltage problems of the grid-tied MG by using reactive power control with considering the limited capacity of the inverters; furthermore, a power curtailment algorithm is proposed in order to mitigate voltage rise problem when the reactive power compensation is not sufficient. The voltage support algorithm is flexible in using central or local measurement of voltage. In addition, a harmonic mitigation method is proposed based on the virtual admittance which has also the flexibility for changing from central measurement to local measurement when the communication system failure happens or the delay of the communication system is too high.

The main contributions of the paper are listed below:

- A coordinated control of CCM VSIs for harmonic compensation and reactive power sharing/support.
- Considering the limited capacity of the inverter in harmonic and reactive power compensation.
- Voltage rise mitigation by using reactive power control and power curtailment of the DG interfacing inverters.
- Flexibility for choosing the local or remote (central) measurement.
- Considering the effect of communication system delay on power quality improvement.

Rest of the paper is presented as follows; Section 2 is focused on the general scheme of the system under study. Section 3 describes the details of the control system. Afterwards, simulation and experimental results are presented in Section 4. Finally, the paper is concluded in Section 5.

2. General scheme of the system

Fig. 1 shows the general overview of the grid-connected MG. As shown in this figure, each CCM VSI (DG_n) which can be considered as interfacing inverter of PV or WT unit is connected to the PCC via impedance (Z_{Ln}). The line impedances are considered resistive in order to simulate the distribution system lines. The MG is connected through a line and a transformer with impedances represented by Z_G and Z_T, respectively. The voltage of PCC bus is measured and the harmonics extraction is achieved using *dq* transformation. In order to increase the reliability of the communication system, low bandwidth communication (LBC) system is used; hence, the transmitted data should be in DC, as the results of the applied extraction method are DC values in *dq* synchronous reference frame. The details of PCC fundamental and harmonics extraction can be found in Ref. [15]. The fundamental and harmonic transmitted data are fed to each DG

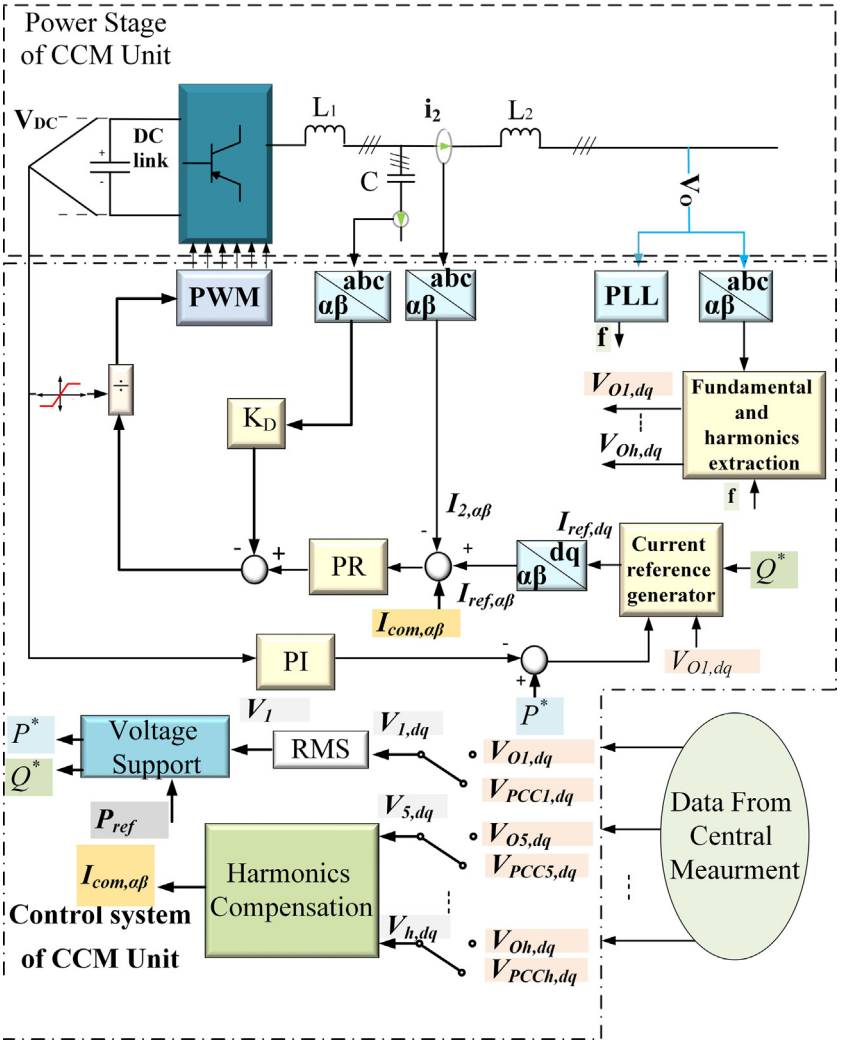

Fig. 2. Power and control stage of DG interfacing inverter.

local controller for voltage support and harmonic compensation, respectively.

3. Control approach for DG interface inverter

Fig. 2 shows the control block of DG interfacing inverter. As mentioned before, the DG interfacing inverters are connected to the MG by using an LCL filter. Harmonic resonance problem can inherently endanger the stability of the system due to the use of LCL filter [23]. Different active and passive methods have been proposed by researchers to solve the resonance problem [24,25]. In this paper, capacitor current feedback is used for damping the resonance (see K_D in Fig. 2). In this control scheme, multi-loop control scheme is used for controlling the injected current of the VSI. The reference power is tracked by the outer loop whereas the stability improvement and resonance damping are carried out through the inner loop [24].

In the outer control loop, Proportional Resonant (PR) controllers which are tuned at fundamental, 5th, 7th and 11th harmonics orders are used. The output voltage of LCL filter (V_o) is used as a feedback. Since this point is closer to the PCC than the filter capacitor, controlling its voltage provides a better voltage quality at PCC [16].

As depicted in Fig. 2, and mentioned before, fundamental component and harmonic orders of PCC voltage are extracted in *dq* frame ($V_{PCC1,dq}$, $V_{PCC5,dq}$, $V_{PCC7,dq}$ and $V_{PCC11,dq}$) and transmitted via the communication system as data from central measurement. However, the local measurements ($V_{O1,dq}$, $V_{O5,dq}$, $V_{O7,dq}$ and $V_{O11,dq}$) can be used if the communication system has a failure or long time delay. Hence, this flexibility can increase the reliability of the system.

In Fig. 2, P_{ref} is the active power that can be injected to the grid. The reference active and reactive powers (P^* and Q^*) and the reference harmonic compensation current ($I_{com,\alpha b}$) are generated by voltage support and harmonics compensation blocks, respectively. After calculation of the reference of active and reactive powers (P^* and Q^*), the fundamental current reference in *dq* frame ($I_{ref,dq}$) is generated by Eq. (1) [26]. Generally DC voltage feedback is used in order to fix the DC bus voltage [26]. Since in this paper, the focus is on the inverter control, a constant DC voltage source is assumed; thus, the DC voltage feedback does not work. In order to prevent of any misunderstanding, the feedback is not considered in this equation:

$$\begin{bmatrix} I_{ref,d} \\ I_{ref,q} \end{bmatrix} = \begin{bmatrix} V_{O1,d} & V_{O1,q} \\ -V_{O1,q} & V_{O1,d} \end{bmatrix}^{-1} \begin{bmatrix} P^* \\ Q^* \end{bmatrix} \quad (1)$$

Division of the DC bus voltage which is applied before PWM block can isolate the tuning of the controller against the DC voltage changes. However, during the startup, since the amount of DC voltage is low, the division to DC voltage can cause a large gain which can lead to instability. In this paper, the measured DC voltage passes through a saturation block whose minimum and maximum values are defined as 0.9 $V_{DC,N}$ and 1.1 $V_{DC,N}$ (where $V_{DC,N}$ represents the nominal value of V_{DC}).

3.1. Voltage support function of the VSI interfacing inverter

Reactive power control is conventionally used for voltage regulation in power systems. Incorporation of the free capacity of DGs inverters is considered as a potential for reactive power compensation and voltage support. Although IEEE 1547 standard [27] forbids the use of reactive power capability of inverter-based DGs for this purpose, this policy would be changed by increasing penetration of DG systems [28].

International Electronical Committee (IEC) 61850-90-7 recommends advanced reactive functions and object models for power converter based Distributed Energy Resources (DERs) [29]. According to this standard, the DG units shall respond to the voltage variation in order to enhance the voltage profile of power system [30]. According to the standard and the method presented in Ref. [3], the reactive power compensation is implemented in this paper.

For achieving this aim, the RMS of fundamental component of the measured voltage is compared to its reference value. Afterward, according to the voltage and the remaining capacity, the reference reactive power of the inverter is generated. The following criteria are utilized to compensate over/under voltage problems by the inverter according to IEC 61850-90-7 [3]:

$$Q^* = \begin{cases} Q_{max} & V < V_1 \\ Q_{max} - \dfrac{Q_{max}}{V_2 - V_1}(V - V_1) & V_1 \le V \le V_2 \\ 0 & V_2 \le V \le V_3 \\ -\dfrac{Q_{max}}{V_4 - V_3}(V - V_3) & V_3 \le V \le V_4 \\ -Q_{max} & V < V_4 \end{cases} \quad (2)$$

where $V_1 = 0.9\ V_r$, $V_2 = 0.95\ V_r$, $V_3 = 1.025\ V_r$ and $V_4 = 1.05\ V_r$. V_r represents the rated voltage of the grid which is equal to 230 V in this paper. The threshold values of $V_1 = 0.9\ V_r$ and $V_4 = 1.05\ V_r$ are determined according to IEEE 1159 standard as minimum and maximum allowable voltages, respectively [31]. According to IEEE 1547 standard, the maximum allowable voltage fluctuation caused by DG is set at 5%. Furthermore, it is compatible with U.S. grid code in which the normal operating range of a PV system is defined in the range of 0.95–1.05 p.u. while in extreme conditions the voltage range of 0.88–1.1 p.u. is defined [5]. However, the maximum value is more restricted than the EN 50160 European standard [32] in which the allowable voltage is in the range of 0.9–1.1 p.u. It should be mentioned that in the above equation, Q_{max} represents the free capacity of the inverter for reactive power compensation which can be written as:

$$Q_{max} = \sqrt{S_r^2 - P^2} \quad (3)$$

Fig. 3 shows the reactive power compensation effort of DG interfacing inverter. As shown in this figure if the RMS value of the measured voltage (V) is higher/lower than V_4/V_1 (standard limitation), all of the capacity will be dedicated to voltage rise/under voltage mitigation. The reactive power injection which changes linearly when V is in the range of $V_1 \le V \le V_2$ or $V_3 \le V \le V_4$.

The method presented in Ref. [3] is only based on local measurements and the voltage rise mitigation is achieved by measuring the voltage of each DG. In this approach, since the different voltages may be measured by each DG in a distribution system, unfair reactive power compensation occurs between DGs. However, in the present paper, when central measurement is used, due to the fact that the PCC voltage information is sent to each DG, the same voltage is measured by DGs and the reactive compensation efforts of DGs are proportional to their capacities. If the communication system fails, the local control can undertake compensation; hence, the reactive power compensation will be active even a communication failure happens.

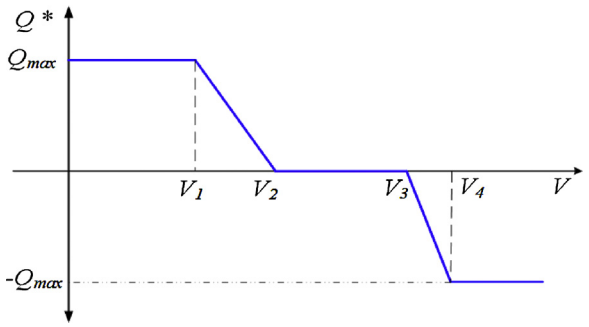

Fig. 3. Reactive power control of DG units.

In Ref. [33], power curtailment approach has been recommended for PV systems in order to overcome the over frequency problem when the consumption is less than the production of DG units in an inductive islanded microgrid. However, in resistive systems, the voltage amplitude is depended on active power; hence, the power curtailment may mitigate the voltage rise problem [4,5]. The presented method in Ref. [4] is based on local measurement and as mentioned before, this method can lead to unfair efforts of DGs due to the measurement of different voltages in each DGs terminal; Furthermore, measuring the PCC voltage can lead to proper reaction to voltage variation of PCC which is the aim of compensation. In the method of Ref. [5], a two-way communication system is required. In comparison to the methods which are proposed in Refs. [4,5], the proposed method in this paper has the flexibility in choosing central (remote) measurement by using only one-way communication system (from PCC to DGs) or local measurement when communication failure happens.

In case of over voltage, the reduction of active power can compensate it if the reactive power support is not sufficient. The following active power curtailment can be applied to the inverter.

$$P^* = \begin{cases} P_{ref} & V < V_5 \\ P_{ref} - K.P_{ref} & V_5 \le V \le V_6 \end{cases} \quad (4)$$

where K is reduction coefficient which is defined as

$$K = \frac{V - V_5}{V_6 - V_5} \quad (5)$$

where $V_5 = 1.05\ V_r$ and $V_6 = 1.1\ V_r$. This voltage rise mitigation approach is depicted in Fig. 4.

In other words, firstly the reactive power compensation is applied to the inverters; afterwards the active power curtailment scenario will be utilized if the reactive power support is not sufficient.

3.2. Harmonics compensation

In this paper, the harmonic compensation function of DG units is also addressed. The harmonic compensation can either be performed based on PCC voltage measurement (central measurement) or local measurement (at the terminal of VSI LCL filter). Virtual admittance is used for harmonic compensation purpose. The lim-

Fig. 4. Voltage rise mitigation by using power curtailment.

ited capacity of the inverter is also considered in current harmonics compensation.

Fig. 5 shows the virtual admittance block. As shown in this figure, after harmonic extraction, individual harmonic indices (H_h) are calculated by division of the RMS amount of each harmonic (V_h) to the RMS fundamental component V_1.

After comparison of H_h to its allowable amount (H_h^*), a deadband block is used in order to prevent the controller to compensate harmonics when the value of H_h is lower than H_h^*. In other words, by using the deadband block the DG does not contribute in harmonics compensation when it is not required. Afterward, a proportional (P) controller is used to regulate controller, since the power curtailment is shared between different DG systems. In order to distribute harmonic compensation effort among DG units, the ratio of DG_i is rated power and the total power of all MG DGs are used as a gain ($S_i/\Sigma S_j$). By using the gain, the DGs with higher rated power contributes more in harmonic compensation.

Note that the H_h^* can be determined based on the sensitivity of the load to harmonics or grid codes and standards.

Fig. 5(b) shows the general overview of harmonic compensation block. The limited capacity of the inverter in harmonics compensation is considered by calculation of maximum admittance. The maximum capacity of the inverter is calculated according to IEEE 1459 standard [34]. The maximum injectable harmonic current can be calculated as follows:

$$I_{H,\max} = \sqrt{I_R^2 - I_{o,1}^2} = \sqrt{G^2_{MAX,H5}V_5{}^2 + G^2_{MAX,H7}V_7{}^2 + \ldots + G^2_{MAX,Hh}V_h{}^2} \quad (6)$$

where I_R represents the RMS of rated current and $I_{O,1}$ is the RMS of fundamental component of DG injected current. The calculated maximum values of virtual admittance are fed to the dynamic limiter blocks. Since Eq. (6) contains more than one unknown parameter, it is assumed that the values of maximum admittance for different frequencies are the same ($G_{MAX,H5} = G_{MAX,H7} = \ldots = G_{MAX,Hh}$); hence $G_{MAX,Hh}$ can be written as

$$G_{MAX,Hh} = \frac{\sqrt{I_R^2}}{V_1\sqrt{H_5{}^2}} \quad (7)$$

As shown in Fig. 3(b), the compensation current at h harmonic ($I_{com,hdq}$) is calculated by multiplying the virtual admittance with corresponding voltage harmonic. Afterward, the compensation current in the dq frame is transformed to the $\alpha\beta$ (stationary)

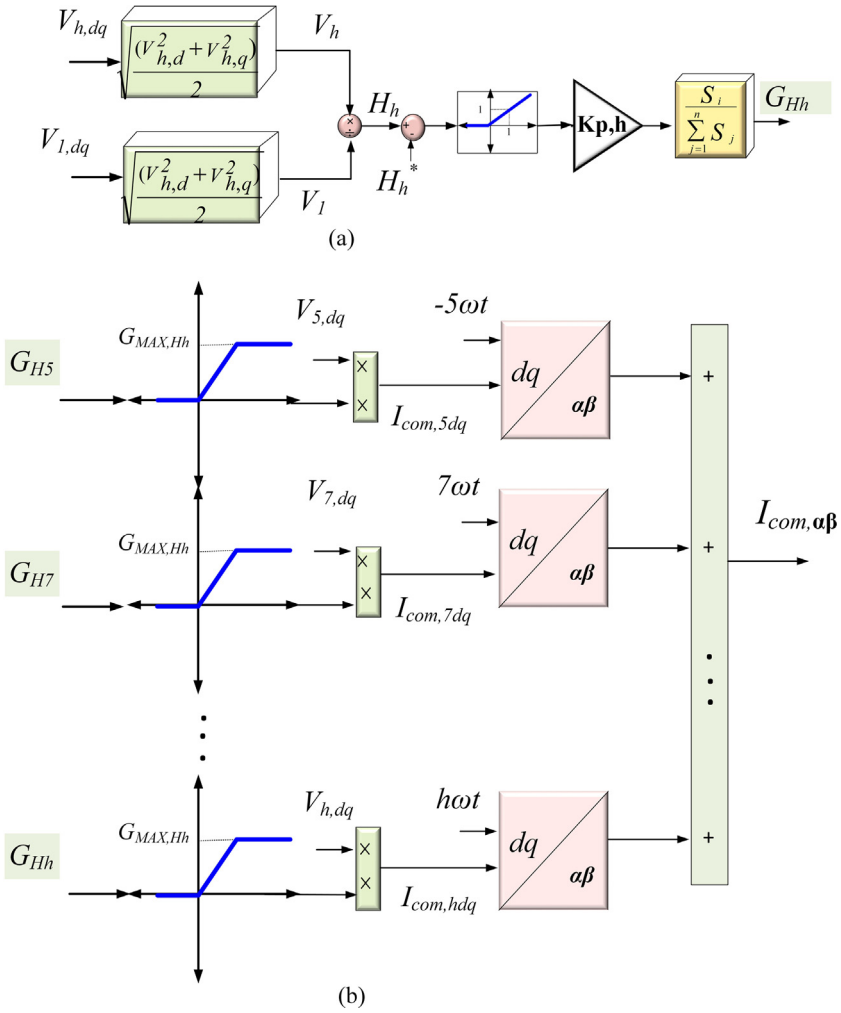

Fig. 5. Details of virtual admittance block of Fig. 2; (a) G_{Hh} calculation block; (b) overall scheme.

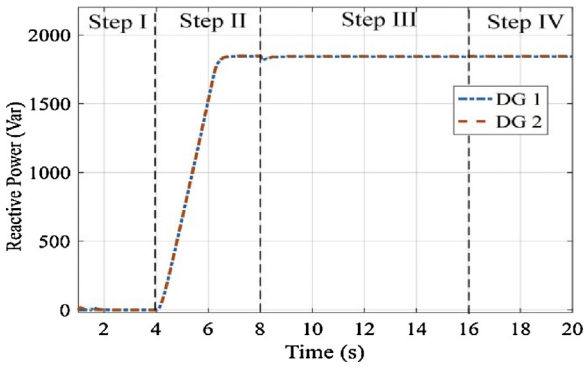

Fig. 6. Reactive power in first scenario.

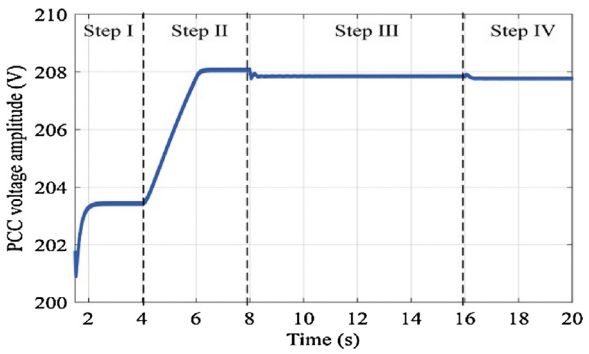

Fig. 7. Voltage amplitude in first scenario.

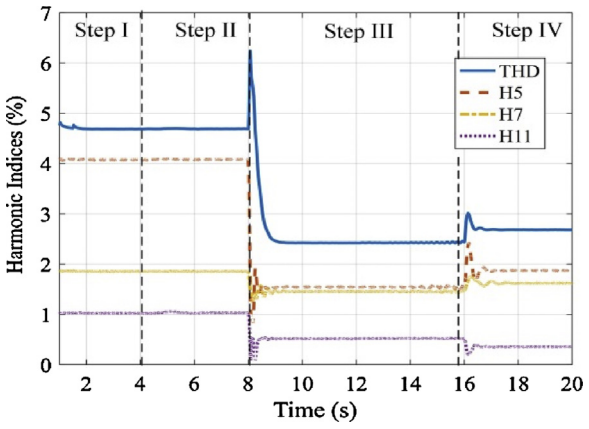

Fig. 8. Harmonic indices of PCC voltage in different steps of first scenario.

frame. Finally, the compensation currents at different frequencies are added together to create the total compensation current ($I_{com,\alpha\beta}$).

4. Simulation and experimental results

The system shown in Fig. 1, with two inverter-based DGs is used as the case study. Each DG is connected to the PCC by using an LCL filters and a distribution line. PCC voltage measurement is implemented and fundamental and harmonics contents of PCC voltage are transferred to each DG by a one-way communication system. The parameters of power and control systems of the case study are listed in Tables 1 and 2, respectively. As it can be found in Table 1, the lines impedances of DG_1 and DG_2 are considered different in order to evaluate the proposed algorithm better; furthermore, it is assumed that the capacities of the inverters are 10% more than their available maximum powers which can be delivered in order to provide some rooms for reactive power and harmonics compensation.

For evaluation of voltage support and harmonic compensation functions, one simulation scenario and two experimental scenarios are studied.

4.1. First scenario (simulation): high consumption and low power injection

In order to evaluate the effectiveness of the method for compensation in voltage drop conditions, the DGs generated powers are assumed to be low (300 W); and a combination of nonlinear and linear loads is considered. The following steps are taken into account:

- Step I ($t < 4s$): without any power quality compensation.
- Step II ($4 \leq t < 8$): voltage support activation.
- Step III ($8 \leq t < 16$): activation of voltage harmonics compensation with central measurement considering 1 ms delay for communication system.
- Step IV ($16 \leq t < 20$): failure of communication system and local measurement based compensation.

Fig. 6 shows the delivered reactive power of DG units while the PCC voltage amplitude is depicted in Fig. 7. As shown in these figures, after activation of voltage support, the PCC under voltage problem is mitigated in Step II (voltage amplitude is about 0.905 V_r in Steps II–IV) by injection of reactive power to the grid. Furthermore, the voltage support is obtained in Steps IV in which the delay and failure of communication system take place. Since the active power of DG units and their related currents are low, the voltage across Z_{L1} and Z_{L2} (see Fig. 1) are low and the amplitudes of PCC and DGs output voltages ($V_{O,1}$ and $V_{O,2}$) are approximately the same; Hence there is no significant different between voltage amplitudes in Steps III and IV where, respectively, PCC voltage measurement and DGs output voltages ($V_{O,1}$ and $V_{O,2}$) are used as input of "Voltage Support" block.

Fig. 8 shows the harmonic content of PCC voltage in different steps. As depicted in Step 2 (only reactive power compensation), the PCC voltage harmonic content is high in this step while undervoltage mitigation occurs in this step. It shows that if the voltage support is the only objective of the controller (the method which is presented in Refs. [3–5]), the harmonic distortion problem should be tackled by using additional dedicated harmonic compensation devices. As depicted in this figure, the PCC voltage compensation is achieved in different steps. The THD of voltage is decreased to 2.5 and 2.8 in Steps III and IV, respectively. It is shows that if the failure of communication system happens, the control system can compensate based on local measurement. This flexibility in choosing local and central measurement is the advantage of the proposed method in comparison with the communication-based methods reported in Refs. [13,15,16]. Fig. 9 shows the PCC voltage before and after compensation (in Steps II and III).

4.2. Second scenario: high generation and low demand (without any load in PCC)

Fig. 10 shows the experimental setup for this study which consist of inverters, dSPACE controller, nonlinear load, distribution line panel and power quality analyzer.

For evaluation of voltage rise mitigation, it is assumed that the power generation is high and there is no local consumption in grid-connected MG. The parameters of the system are listed in Table 1. The diagram of the system is similar to the first scenario without

Table 1
Power stage parameters.

DC link voltage	LCL filter (L_1/C/L_2)	Voltage/frequency
700 V	For all DGs: 8.6 mH/4.5 μF/1.8 mH	230 V/50 Hz

Nonlinear Load			Linear load (simulation)	Linear load (experimental)
C_{NL} (μF)	R_{NL} (Ω)	L_{NL} (mH)	Z_L (Ω)	Z_L (Ω)
235	114	0.084	18 + 100j	No load

Line impedance		
Z_{L1} (Ω)	Z_{L2} (Ω)	Z_{NL} (Ω)
0.66	1	0.1 + 0.5j

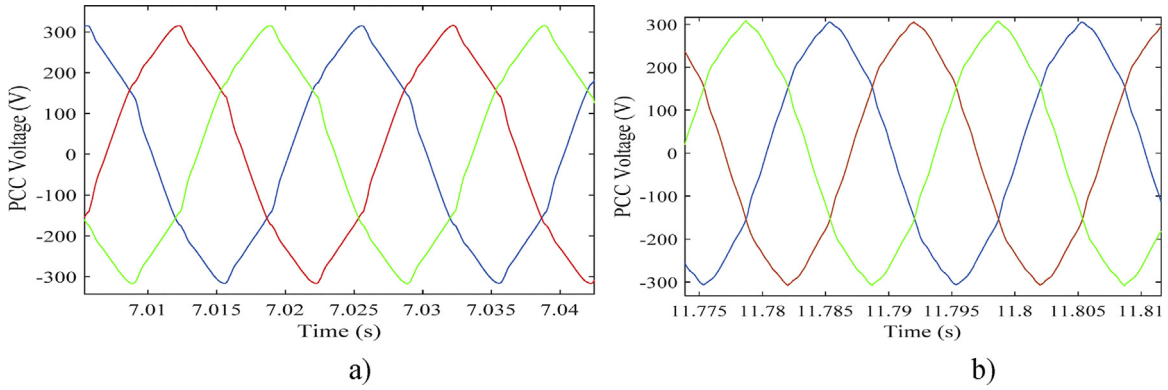

Fig. 9. PCC voltage in first scenario, (a) before compensation (in Step II), (b) after compensation (in Step III).

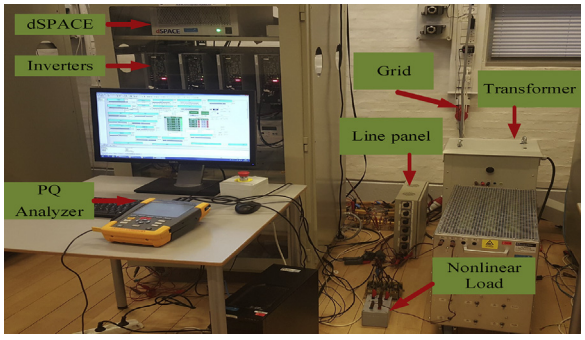

Fig. 10. Experimental setup of the grid tied inverters.

any local load in order to evaluate the effectiveness of the method in voltage rise mitigation. The following steps are considered:

- Step A: integration of DGs without voltage support.
- Step B: activation of voltage support by using central measurement and deactivation power curtailment algorithm.
- Step C: failure of communication system and activation of voltage support using local measurement.
- Step D: activation of voltage support using local measurement and activation of power curtailment algorithm.
- Step E: activation of voltage support using remote (at PCC) measurement and activation of power reduction.

The test is implemented when the grid voltage is approximately 231 V. Active and reactive powers which are delivered by DGs and amplitudes of PCC and output voltage of DGs are depicted in Fig. 11. As depicted in Fig. 11(a), both of these DGs can deliver their reference powers (the value 2000 W) to the grid in Step A. In this step,

Table 2
Control parameters.

Virtual admittance controller					
Allowable individual harmonic (%)			P controllers		
H_5^*	H_7^*	H_{11}^*	$K_{P,5}$	$K_{P,7}$	$K_{P,11}$
1.5%	1%	0.5%	100	100	100

since high power and current are injected to the grid, voltage rise takes place in PCC and output voltages of DGs. Due to the high injected current and the high line resistances of Z_{L1} and Z_{L2}, the voltage rise of output voltages of DGs are higher than the PCC voltage. After activation of the reactive power compensation and using PCC voltage amplitude as the input of "Voltage Support" blocks in Step B, the PCC voltage rise mitigation is achieved and the PCC voltage amplitude is lower than the limit of 1.05 V_r which is determined in Section 3.1, as depicted in Fig. 11(a); however, the amplitudes of the DGs output voltage are higher than the standard limit. The figure also shows that in the case the local measurement is used in Step C, since the output voltages of both DGs are higher than 1.05 V_r, all of their free capacities are dedicated to reactive power compensation.

After activation of power curtailment method and using output voltages of DGs as local measurement in Step D, the power curtailment takes place. In this step, the active power of DGs are decreased because, only the reactive power compensation alone is not sufficient for voltage rise mitigation of the output voltages of DGs. The power curtailment of DG_2 is higher than DG_1. This is attributed to the higher voltage of DG_2 in respect to DG_1 due to the higher line resistance of DG_2. In this step, due to the occurrence of power curtailment, the available reactive power increases according to Eq. (2); furthermore, it shows that if local measurement is used, the

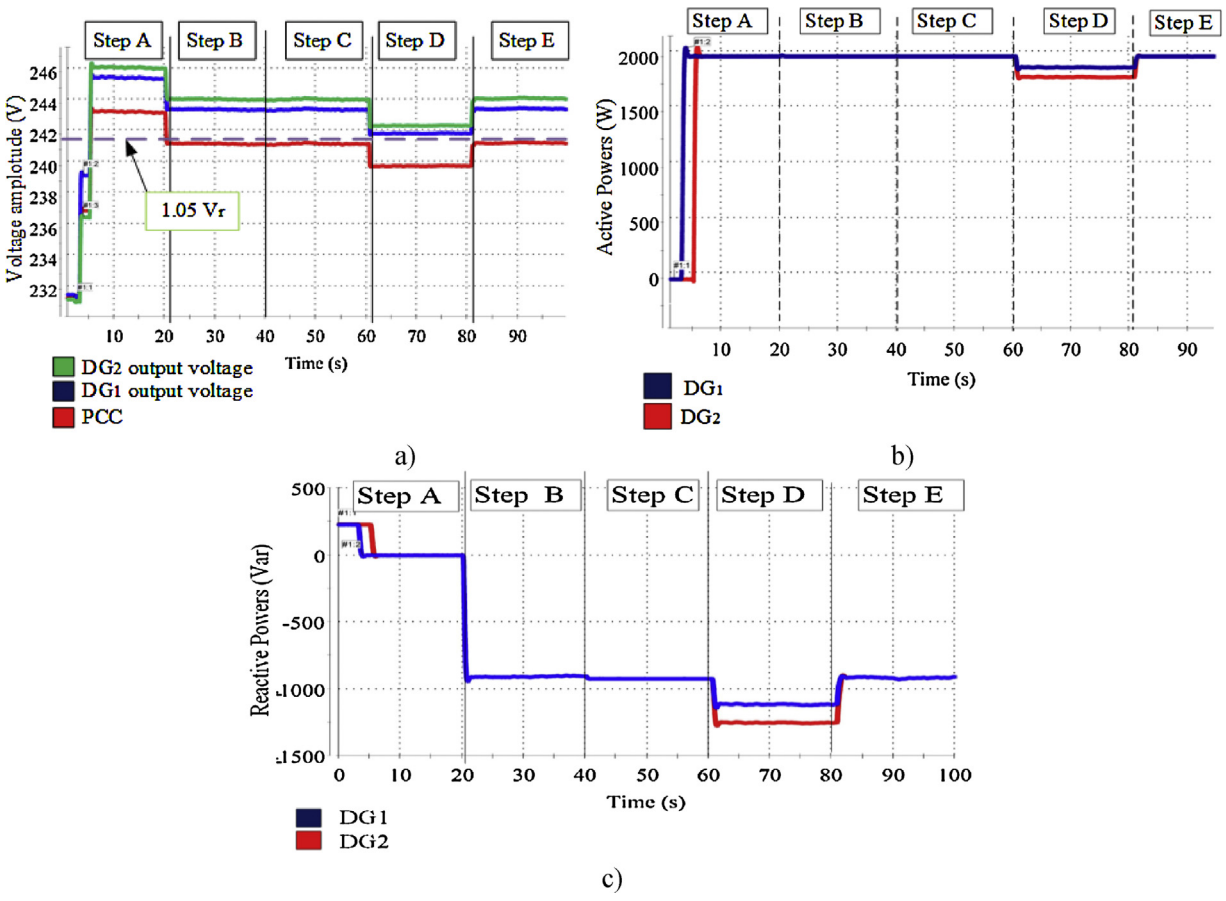

Fig. 11. Experimental results in second scenario with 231 V grid voltage, (a) voltage amplitude, (b) active power, (c) reactive power.

power curtailment is unfair between DGs due to different voltage measurement of DGs.

After reactivation of the communication system in Step E, the power curtailment does not happen because the reactive power compensation is enough to recover the PCC voltage as depicted in Fig. 11(a) and the PCC voltage amplitude is under the *1.05 V_r* which is defined as threshold of power curtailment algorithm according to Fig. 4. It shows that using the PCC voltage measurement can provide a real evaluation of the voltage rise problem in PCC and can prevent the unnecessary compensation as reported in Step D and is used in Ref. [4].

In order to shows the effect of grid voltage on the voltage rise of PCC, another experimental test is performed with the grid voltage of 233 V. Fig. 12 shows the performance of the proposed method in voltage rise mitigation. Fig. 12(a) shows the PCC, DG_1 and DG_2 output voltages. The voltage amplitudes in Fig. 12(a) are higher than those of Fig. 11(a), because of higher grid voltage. Furthermore, as depicted in Fig. 12(a) and (b), after activation of reactive power compensation in Steps b and c, although all of the remaining capacity of DGs are dedicated to reactive power compensation, the PCC and DGs output voltages are higher than 1.05 V_r. After activation of power curtailment method in Step D and using local measurement same as the methods proposed in Ref. [4], since the voltage rise in this case is more severe than the previous one, the power curtailments of DGs are also higher. It also shows that an unfair power curtailment happens because of different local measurements of DGs output voltages. After activation of the one-way communication system in Step E, a fair power curtailment happens for DG_1 and DG_2.

4.3. Third scenario: high generation and medium demand (with nonlinear load)

In this case, a nonlinear load is connected to the PCC bus in order to experimentally validate the harmonic compensation and reactive power support when the load is not as high as the first scenario and only nonlinear load is connected in PCC; the parameters of the nonlinear load are also listed in Table 1.

For evaluation of harmonic compensation, it is assumed that firstly the communication system is working properly with t = 5 ms delay. After that, the communication system fails and the local measurement is activated instead of the remote one.

Fig. 13(a) shows the voltage waveform of PCC before compensation while the measured harmonic content is depicted in Fig. 13(b). As shown in Fig. 13(b), the THD and 5th order harmonic exceeds 5% and 3%, respectively, which are defined as allowable values according to IEEE 519 standard [35].

Fig. 14 shows the PCC voltage waveform and its harmonics contents after compensation considering t = 5 ms delay time. As depicted in Fig. 14(b), the harmonic compensation is achieved and the amounts of harmonics contents are below the limits of IEEE 519 standard.

Fig. 15 shows the PCC voltage waveform and its harmonic content after communication failure. As observed, by using local measurement, in the case of remote (at PCC) measurement, the voltage harmonic compensation is achieved; however, the compensation was more effective by increasing the time delay of communication system, the harmonic content of PCC voltage increases as presented in Table 3. Also, it can be observed that

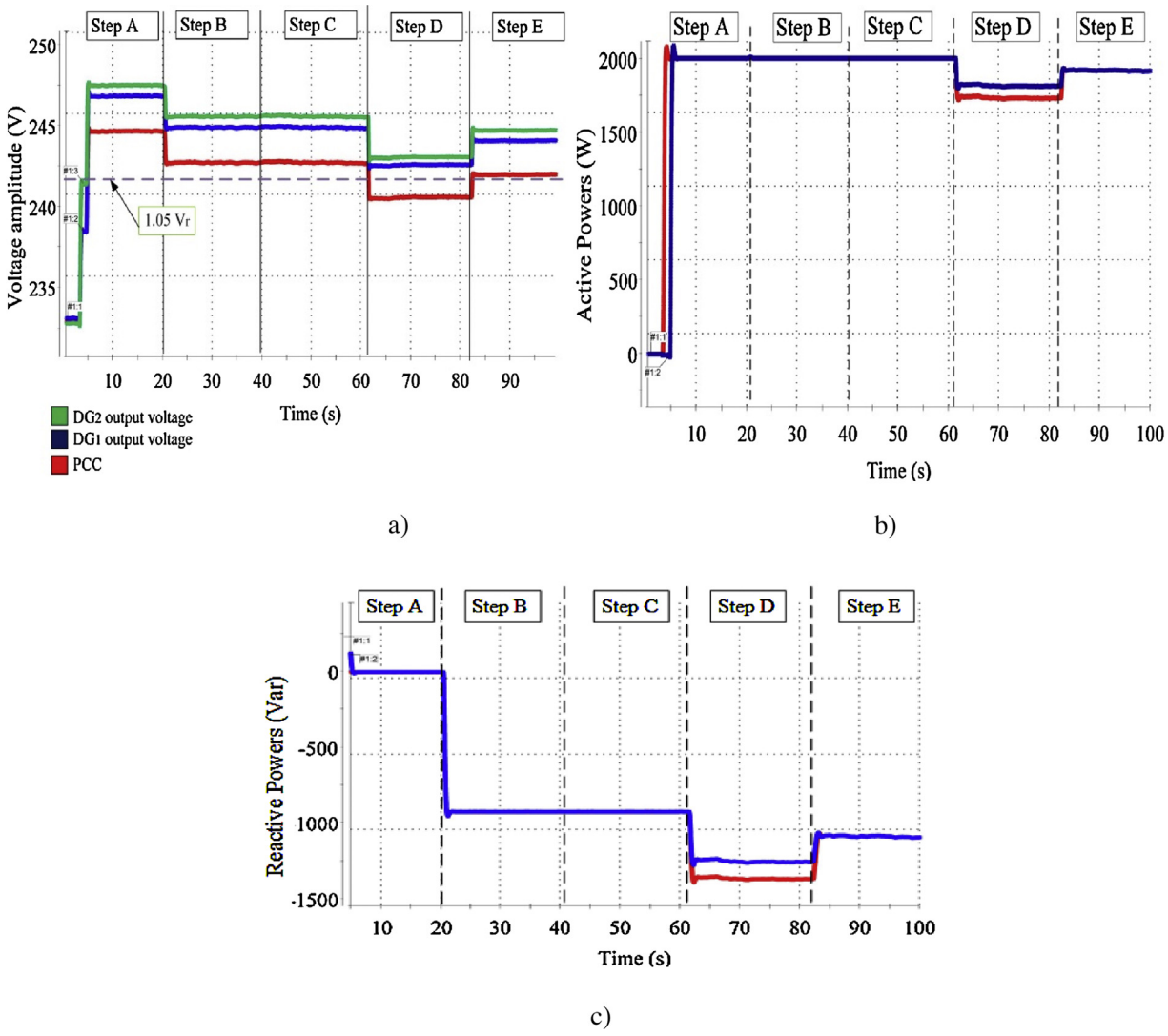

Fig. 12. Experimental results in second scenario with 233 V grid voltage, (a) voltage amplitude, (b) active power, (c) reactive power.

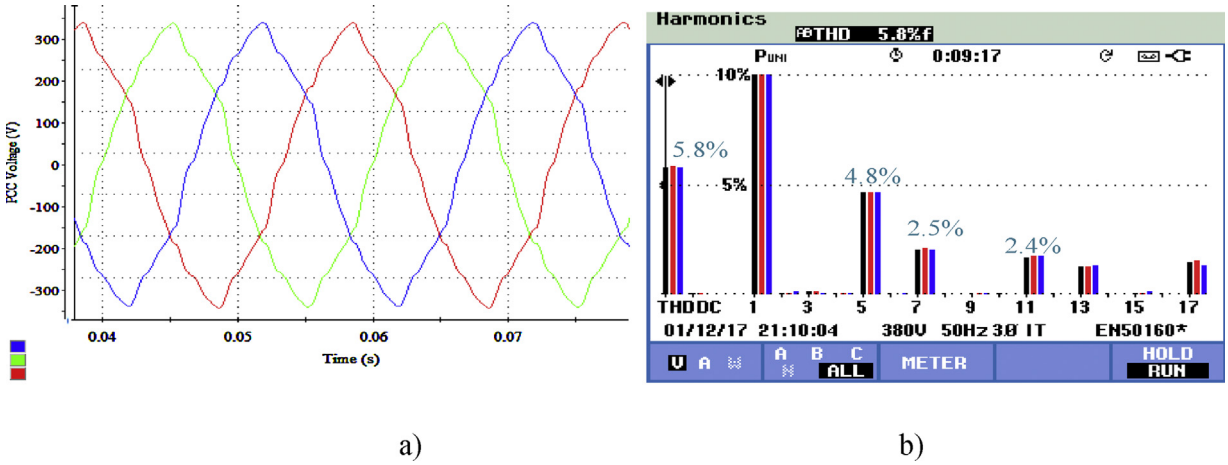

Fig. 13. PCC voltage before harmonic compensation in third scenario (experimental results), (a) voltage waveform, (b) harmonic content.

the local measurement based compensation (the results shown in Fig. 15) can be more effective than the remote measurement case when the delay of communication system is too high (for instance 50 ms).

For evaluation of reactive power control in this scenario, three following steps are implemented:

- Step a: without reactive power compensation.
- Step b: reactive power compensation without communication system.
- Step c: reactive power compensation with communication system.

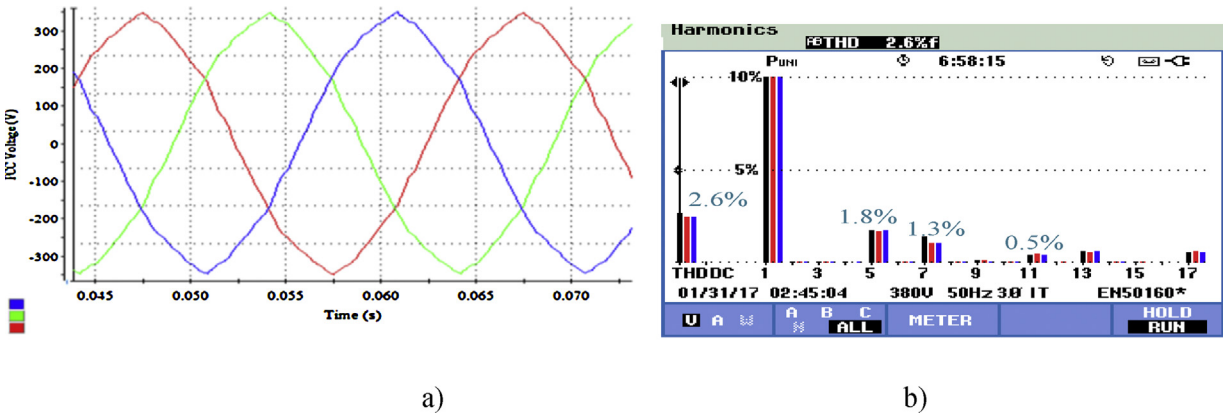

Fig. 14. PCC voltage, with communication system and 5 ms delay in third scenario (experimental results) (a) voltage waveform, (b) harmonic content.

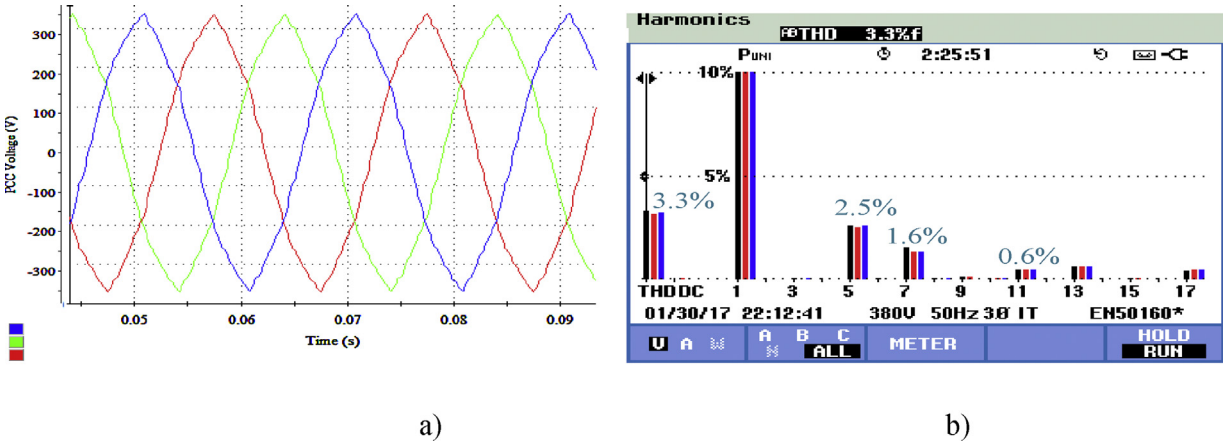

Fig. 15. PCC voltage without communication system third scenario (experimental results) (a) voltage waveform, (b) harmonic content.

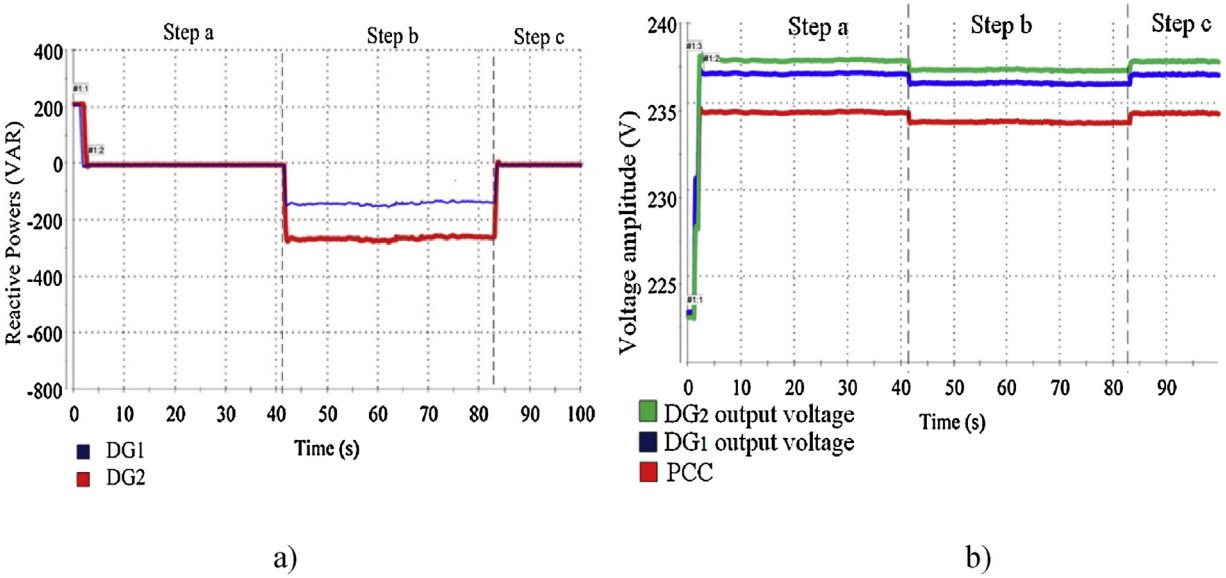

Fig. 16. Experimental results for third scenario (a) reactive power, (b) voltage amplitude.

Fig. 16(a) shows the reactive power delivered by DG units while the RMS fundamental voltage of PCC and output voltage of DGs are depicted in Fig. 16(b). As can be seen in Fig. 16(a), when the local measurement is available (in Step b), the DG units contribute in voltage rise mitigation by absorbing reactive power. The reactive power compensation is stopped in Step c where the remote measurement is used, because the measured voltage of PCC shows that the amplitude is lower than 1.025 V_1 (below the limit as defined in Eq. (2)) and thus, the voltage rise mitigation is not necessarily needed; whereas in Step b the local measurements have shown the necessity of compensation.

Table 3
Harmonics indexes in experimental study.

Delay time	Harmonics indexes			
	THD (%)	H_5 (%)	H_7 (%)	H_{11} (%)
0.5 ms	2.4	1.5	1.1	0.5
10 ms	3.1	2.4	1.5	0.5
50 ms	3.7	2.9	1.7	0.6
Local measurement	3.3	2.5	1.6	0.6

5. Conclusions

In this paper, the contribution of DGs in voltage support and harmonic compensation in a grid-connected MG is investigated. Both of voltage support and harmonics compensation can be chosen by local or communication-based measurement and the limited capacity of the DG interfacing inverters is also considered in voltage support and harmonics compensation.

The proposed harmonic compensation is based on virtual admittance and has the flexibility in selecting local or remote measurement. The limited capacity of inverter and the effect of communication system delay have been investigated. Experimental and simulation results show that after harmonics compensation, the amounts of individual harmonics and THD are less than their allowed values according to IEEE 519 and EN 50160 standards. The study has also shown that compensation based on central (remote) measurement will be more effective than local-measurement-based compensation if the commutation system delay is low.

Furthermore, over/under voltage compensation by the DG units has been assessed. The voltage rise mitigation is achieved by active and/or reactive power curtailment with the flexibility for remote or local measurement. The active power curtailment is used when reactive power compensation is not sufficient for voltage rise control. Furthermore, the under voltage compensation is achieved by injecting reactive power with considering the limited capacity of the inverter. The results showed that if only the local measurement is available and the PCC voltage quality improvement is considered as the main goal of compensation, unnecessary compensation can be avoided. The reliability of the system can be increased when a communication failure occurs.

References

[1] T.C. Green, M. Prodanović, Control of inverter-based micro-grids, Electr. Power Syst. Res. 77 (2007) 1204–1213.
[2] Pedro M.S. Carvalho, Pedro F. Correia, Luís A.F.M. Ferreira, Distributed reactive power generation control for voltage rise mitigation in distribution networks, IEEE Trans. Power Syst. 23 (2) (2008) 766–772.
[3] Erhan Demirok, et al., Local reactive power control methods for overvoltage prevention of distributed solar inverters in low-voltage grids, IEEE J. Photovolt. 1 (2) (2011) 174–182.
[4] Mohammad Amin Ghasemi, Mostafa Parniani, Prevention of distribution network overvoltage by adaptive droop-based active and reactive power control of PV systems, Electr. Power Syst. Res. 133 (2016) 313–327.
[5] S. Alyami, W. Yang, W. Caisheng, Z. Junhui, Z. Bo, Adaptive real powercapping method for fair overvoltage regulation of distribution networkswith high penetration of PV systems, IEEE Trans. Smart Grid 5 (2014) 2729–2738.
[6] Arash Momeneh, et al., Comparative study of reactive power control methods for photovoltaic inverters in low-voltage grids, IET Renew. Power Gener. 10 (3) (2016) 310–318.
[7] Yongheng Yang, et al., Power control flexibilities for grid-connected multi-functional photovoltaic inverters, IET Renew. Power Gener. 10 (4) (2016) 504–513.
[8] Pedro G. Bueno, Jesus C. Hernández, Francisco J. Ruiz-Rodriguez, Stability assessment for transmission systems with large utility-scale photovoltaic units, IET Renew. Power Gener. 10 (5) (2016) 584–597.
[9] C. Hernandez Jesus, G. Bueno Pedro, Francisco Sanchez-Sutil, Enhanced utility-scale photovoltaic units withfrequency support functions and dynamic grid support for transmission systems, IET Renew. Power Gener. 11 (3) (2017) 361–372.
[10] Yun Wei Li, Ching-Nan Kao, An accurate power control strategy for power-electronics-interfaced distributed generation units operating in a low-voltage multibus microgrid, IEEE Trans. Power Electron. 24 (12) (2009) 2977–2988.
[11] Juan C. Vasquez, et al., Voltage support provided by a droop-controlled multifunctional inverter, IEEE Trans. Ind. Electron. 56 (11) (2009) 4510–4519.
[12] Z. Zeng, H. Yang, S. Tang, R. Zhao, Objective-oriented power quality compensation of multifunctional grid-tied inverters and its application in microgrids, IEEE Trans. Power Electron. 30 (March (3)) (2015) 1255–1265.
[13] M. Savaghebi, A. Jalilian, J.C. Vasquez, J.M. Guerrero, Secondary control for voltage quality enhancement in microgrids, IEEE Trans. Smart Grid 3 (December (4)) (2012) 1893–1902.
[14] M. Savaghebi, Q. Shafiee, J.C. Vasquez, J.M. Guerrero, Adaptive virtual impedance scheme for selective compensation of voltage unbalance and harmonics in microgrids, in: 2015 IEEE Power & Energy Society General Meeting, Denver, CO, 2015, pp. 1–5.
[15] M. Savaghebi, J.C. Vasquez, A. Jalilian, Josep M. Guerrero, Tzung-Lin Lee, Selective compensation of voltage harmonics in grid-connected microgrids, Math. Comput. Simul. 91 (2013) 221–228.
[16] C. Blanco, D. Reigosa, J.C. Vasquez, J.M. Guerrero, F. Briz, Virtual admittance loop for voltage harmonic compensation in microgrids, IEEE Trans. Ind. Appl. 52 (July–August (4)) (2016) 3348–3356.
[17] Mohammad M. Hashempour, et al., A control architecture to coordinate distributed generators and active power filters coexisting in a microgrid, IEEE Trans. Smart Grid 7 (5) (2016) 2325–2336.
[18] X. Wang, F. Blaabjerg, Z. Chen, Synthesis of variable harmonic impedance in inverter-interfaced distributed generation unit for harmonic resonance damping throughout a distribution network, IEEE Trans. Ind. Appl. 48 (July/August (4)) (2012) 1407–1417.
[19] Xiongfei Wang, F. Blaabjerg, Zhe Chen, Autonomous control of inverter-interfaced distributed generation units for harmonic current filtering and resonance damping in an islanded microgrid, IEEE Trans. Ind. Appl. 50 (January–February (1)) (2014) 452–461.
[20] Mohsen Hamzeh, Houshang Karimi, Hossein Mokhtari, Harmonic and negative-sequence current control in an islanded multi-bus MV microgrid, IEEE Trans. Smart Grid 5 (1) (2014) 167–176.
[21] A. Micallef, M. Apap, C. Spiteri-Staines, J.M. Guerrero, Mitigation of harmonics in grid-connected and islanded microgrids via virtual admittances and impeedances, IEEE Trans. Smart Grid (November (99)) (2015) 1–11.
[22] Zeng Zheng, Rongxiang Zhao, Huan Yang, Coordinated control of multi-functional grid-tied inverters using conductance and susceptance limitation, IET Power Electron. 7 (July (7)) (2014) 1821–1831.
[23] Trung Nhan Nguyen, An Luo, Mingfei Li, A simple and robust method for designing a multi-loop controller for three-phase VSI with an LCL-filter under uncertain system parameters, Electr. Power Syst. Res. 117 (2014) 94–103.
[24] Ch. Bao, X. Ruan, X. Wang, W. Li, D. Pan, K. Weng, Step-by-step controller design for LCL-type grid-connected inverter with capacitor–current-feedback active-damping, IEEE Trans. Power Electron. 29 (March (3)) (2014).
[25] R. Peña-Alzola, M. Liserre, F. Blaabjerg, R. Sebastián, J. Dannehl, F.W. Fuchs, Analysis of the passive damping losses in LCL-filter-based grid converters, IEEE Trans. Power Electron. 28 (6) (2013) 2642–2646.
[26] R. Teodorescu, M. Liserre, P. Rodriguez, Grid Converters for Photovoltaic and Wind Power Systems, vol. 29, John Wiley & Sons, 2011.
[27] IEEE 1547, IEEE Standard for Interconnecting Distributed Resources with Electric Power Systems, 2004.
[28] IEEE SCC21 1547 Standards Development P1547a – Amendment 1 to IEEE Std1547 Working Group Meeting Minutes for June 13–14, 2013, Golden, CO, USA. Available from: http://grouper.ieee.org/.
[29] IEC/TR 61850-90-7, Communication Networks and Systems for Power Utility Automation—Part 90-7: Object Models for Power Converters in Distributed Energy Resources (DER) Systems, IEC, Geneva, Switzerland, 2013.
[30] Yun-Su Kim, et al., New requirements of the voltage/VAR function for smart inverter I distributed generation control, Energies 9 (11) (2016) 929.
[31] IEEE Recommended Practice for Monitoring Electric Power Quality, IEEE Std 1159-2009.
[32] EN 50160 standard, Voltage characteristics of electricity supplied by public distribution systems, 1999.
[33] Dan Wu, et al., Autonomous active power control for islanded ac microgrids with photovoltaic generation and energy storage system, IEEE Trans. Energy Convers. 29 (4) (2014) 882–892.
[34] IEEE Standard Definitions for the Measurement of Electric Power Quantities Under Sinusoidal, Nonsinusoidal, Balanced, or Unbalanced Conditions, IEEE Std 1459-2010 (Revision of IEEE Std 1459-2000), pp. 1–50, March 19 2010.
[35] IEEE 519 Standard, IEEE Recommended Practice and Requirements for Harmonic Control in Electric Power Systems, 2014.